Translational Science

Cancer Research

Early Noninvasive Detection of Response to Targeted Therapy in Non–Small Cell Lung Cancer

Jillian Phallen[1], Alessandro Leal[1], Brian D. Woodward[2], Patrick M. Forde[1], Jarushka Naidoo[1], Kristen A. Marrone[1], Julie R. Brahmer[1], Jacob Fiksel[1], Jamie E. Medina[1], Stephen Cristiano[1], Doreen N. Palsgrove[1], Christopher D. Gocke[1], Daniel C. Bruhm[1], Parissa Keshavarzian[2], Vilmos Adleff[1], Elizabeth Weihe[2], Valsamo Anagnostou[1], Robert B. Scharpf[1], Victor E. Velculescu[1], and Hatim Husain[2]

Abstract

With the advent of precision oncology, there is an urgent need to develop improved methods for rapidly detecting responses to targeted therapies. Here, we have developed an ultrasensitive measure of cell-free tumor load using targeted and whole-genome sequencing approaches to assess responses to tyrosine kinase inhibitors in patients with advanced lung cancer. Analyses of 28 patients treated with anti-EGFR or HER2 therapies revealed a bimodal distribution of cell-free circulating tumor DNA (ctDNA) after therapy initiation, with molecular responders having nearly complete elimination of ctDNA (>98%). Molecular nonresponders displayed limited changes in ctDNA levels posttreatment and experienced significantly shorter progression-free survival (median 1.6 vs. 13.7 months, $P < 0.0001$; HR = 66.6; 95% confidence interval, 13.0–341.7), which was detected on average 4 weeks earlier than CT imaging. ctDNA analyses of patients with radiographic stable or nonmeasurable disease improved prediction of clinical outcome compared with CT imaging. These analyses provide a rapid approach for evaluating therapeutic response to targeted therapies and have important implications for the management of patients with cancer and the development of new therapeutics.

Significance: Cell-free tumor load provides a novel approach for evaluating longitudinal changes in ctDNA during systemic treatment with tyrosine kinase inhibitors and serves an unmet clinical need for real-time, noninvasive detection of tumor response to targeted therapies before radiographic assessment.

See related commentary by Zou and Meyerson, p. 1038

Introduction

The management of oncogene-addicted cancer has been improved by the development of targeted therapies that act against a variety of cancer dependencies (1, 2). However, therapeutic efficacy of targeted therapies has been limited by incomplete pharmacologic suppression of tumors or through the selection of resistance mutations in subclonal populations of tumor cells. Disease monitoring using CT imaging is the current clinical practice for assessing response to targeted therapy, yet this approach does not fully represent the molecular and pathologic changes occurring in tumors during therapy. Repeat tissue biopsies of accessible cancer lesions have been used to provide insights into therapeutic decision-making but rarely capture the complexity of intra- and intertumoral heterogeneity and are invasive procedures with potential complications. Theoretically, the ability to noninvasively track specific clonal populations of tumor cells over time has the potential to rapidly and dynamically inform therapy sequence and combinatorial strategies. However, there are currently no approved or clinically recognized noninvasive molecularly defined strategies to assess early drug responsiveness or adaptive resistance in patients with cancer before radiographic progression.

Cell-free circulating tumor DNA (ctDNA) is released from tumor cells into the circulation and has been detected in patients with early- and late-stage cancers (3–8). A key challenge of liquid biopsy approaches has been developing methods to detect and characterize small fractions of ctDNA in large populations of total cell-free DNA. A variety of studies have focused on changes in ctDNA during the course of therapy, but have largely focused on the analysis of specific or limited number of alterations that may only represent specific subclones of the tumor (9–18). More recent studies have used panels of commonly mutated driver genes to allow detection of multiple driver clones, typically at the time of diagnosis (4, 6, 19–21). However, no study has yet assessed the clinical value of a comprehensive genome-wide analysis of ctDNA alterations to evaluate tumor burden at very early timepoints following commencement of targeted therapy.

[1]The Sidney Kimmel Comprehensive Cancer Center, Johns Hopkins University School of Medicine, Baltimore, Maryland. [2]Division of Hematology and Oncology, Moores Cancer Center, University of California, San Diego, La Jolla, California.

Note: Supplementary data for this article are available at Cancer Research Online (http://cancerres.aacrjournals.org/).

J. Phallen, A. Leal, and B.D. Woodward are the co-first authors of this article.

Corresponding Authors: Victor E. Velculescu, The Sidney Kimmel Comprehensive Cancer Center, Johns Hopkins University School of Medicine, 1550 Orleans St, Rm 544, Baltimore, MD 21287. Phone: 410-955-7033; Fax: 410-502-5742; E-mail: velculescu@jhmi.edu; and Hatim Husain, Division of Hematology and Oncology, Moores Cancer Center, University of California San Diego, 3855 Health Sciences Dr #0987, La Jolla, CA 92093. Phone: 858-822-6100; E-mail: hhusain@ucsd.edu

doi: 10.1158/0008-5472.CAN-18-1082

We hypothesized that kinetic changes in the amount of DNA released from tumor cells may occur within hours to days of treatment administration. In this study, we used an ultrasensitive liquid biopsy approach to evaluate patients with advanced non–small cell lung cancer who had tumor responses or progression on tyrosine kinase inhibitors, including erlotinib, a first-generation inhibitor of the EGFR, afatinib, a second-generation inhibitor of EGFR, and ERBB2 (22–24), as well as osimertinib and mavelertinib (PF-06747775), third-generation tyrosine kinase inhibitors targeting EGFR with activating and resistance (T790M) mutations (25, 26). Overall, these analyses investigated whether rapid changes and the overall levels in the amounts of ctDNA can serve as real-time and predictive biomarkers of patient outcome to a targeted cancer therapy.

Patients and Methods

Study design

In this proof-of-principle retrospective study, we assessed serial blood draws from 28 patients with advanced non-small cell lung cancer (NSCLC) undergoing treatment with targeted tyrosine kinase inhibitors (TKI) to directly detect somatic sequence and structural alterations in cfDNA, monitor ctDNA dynamics during therapy, determine cell-free tumor burden, and predict clinical outcome (Fig. 1). Liquid biopsies were obtained immediately prior to treatment (baseline) and at serial timepoints until disease progression. This cohort included 12 patients with RECIST 1.1 partial response, 8 with stable disease, 5 with progressive disease, and 3 with nonmeasurable disease but who derived clinical benefit. We used the ultrasensitive, targeted error correction sequencing (TEC-Seq) approach (6) as well as whole-genome sequencing to identify tumor-derived sequence alterations and chromosomal copy number changes in cfDNA. We evaluated the dynamics of alterations identified and developed a noninvasive measure of cell-free tumor load (cfTL) to evaluate real-time response to treatment. We analyzed changes in cfTL within hours to days after treatment compared with baseline and assessed whether cfTL could serve as a marker of patient outcome.

Patient and sample characteristics

Twenty-eight patients with metastatic non–small cell lung cancer undergoing treatment with TKIs at University of California San Diego (San Diego, CA) or Johns Hopkins University (Baltimore, MD) were included in our study. Clinical and pathologic characteristics for all patients are summarized in Table 1 and Supplementary Tables S1 and S2, and tumor load dynamics are shown in Fig. 2 and in Supplementary Fig. S1. Patient enrollment and genomic studies were conducted in accordance with the Declaration of Helsinki, were approved by the Institutional Review Board and patients provided written informed consent for sample acquisition for research purposes.

The Response Evaluation Criteria in Solid Tumors (RECIST) version 1.1 (27) were used for assessment of response. Of these 28 patients, 20 eventually experienced disease progression while 8 continue to derive clinical benefit from targeted inhibition (Supplementary Table S1).

For all patients, serial blood draws were collected over the course of treatment with targeted inhibition for isolation of plasma and extraction of cfDNA for genomic analyses. Timepoints were analyzed immediately prior to treatment for baseline assessment as well as at serial intervals until disease progression (Supplementary Table S2).

Sample preparation and next-generation sequencing of cfDNA

Whole blood was collected in K2 EDTA tubes or Streck tubes and processed immediately or within 2 hours after storage at 4°C for EDTA tubes or room temperature for Streck tubes, respectively. Plasma and cellular components were separated by centrifugation at 800 × *g* for 10 minutes at 4°C. Plasma was centrifuged a second time at 18,000 × *g* at room temperature to remove any remaining cellular debris and stored at −80°C until the time of DNA extraction. DNA was isolated from plasma using the Qiagen Circulating Nucleic Acids Kit (Qiagen GmbH) and eluted in LoBind tubes (Eppendorf AG). Concentration and quality of cfDNA was assessed using the Bioanalyzer 2100 (Agilent Technologies).

TEC-Seq next-generation sequencing cell-free DNA libraries were prepared from 11 to 350 ng of cfDNA. Genomic libraries were prepared as described previously (6). Briefly, the NEBNext DNA Library Prep Kit for Illumina (New England Biolabs) was used with four main modifications to the manufacturer's guidelines: (i) The library purification steps utilized the on-bead Ampure XP approach, (ii) reagent volumes were adjusted accordingly to accommodate the on-bead strategy, (iii) a pool of 8 unique Illumina dual index adapters with 8-bp barcodes were used in the ligation reaction, and (iv) cfDNA libraries were amplified with Hotstart Phusion Polymerase. Genomic library preparation was performed as described previously (6). Concentration and quality of cfDNA genomic libraries were assessed using the Bioanalyzer 2100 (Agilent Technologies).

Targeted capture was performed using the Agilent SureSelect reagents and a custom set of hybridization probes targeting 58 genes (Supplementary Table S3) as per the manufacturer's guidelines. The captured library was amplified with HotStart Phusion Polymerase (New England Biolabs). The concentration and quality of captured cfDNA libraries were assessed on the Bioanalyzer (Agilent Technologies). TEC-Seq libraries were sequenced using 100-bp paired-end runs on the Illumina HiSeq 2500 (Illumina).

Primary processing of next-generation sequencing data and identification of putative somatic mutations

Primary processing of next-generation sequence data for analyses of sequence alterations in cfDNA samples was performed as described previously (6). Briefly, Illumina CASAVA (Consensus Assessment of Sequence and Variation) software (version 1.8) was used for demultiplexing and masking of dual index adapter sequences. Sequence reads were aligned against the human reference genome (hg19) using NovoAlign with additional realignment of select regions using the Needleman–Wunsch method (28).

Candidate somatic mutations, consisting of point mutations, small insertions, and deletions were identified using VariantDx (28) across the targeted regions of interest as described previously (6).

Briefly, an alteration was considered a candidate somatic mutation only when: (i) three distinct paired reads contained the mutation in the plasma and the number of distinct paired reads containing a particular mutation in the plasma was at least 0.1% of the total distinct read pairs; or (ii) four distinct paired reads contained the mutation in the plasma and the number of distinct paired reads containing a particular mutation in the plasma was at least 0.05% and less than 0.1% of the total distinct read pairs; (iii) the mismatched base was not present in >1% of the reads in a panel of unmatched normal

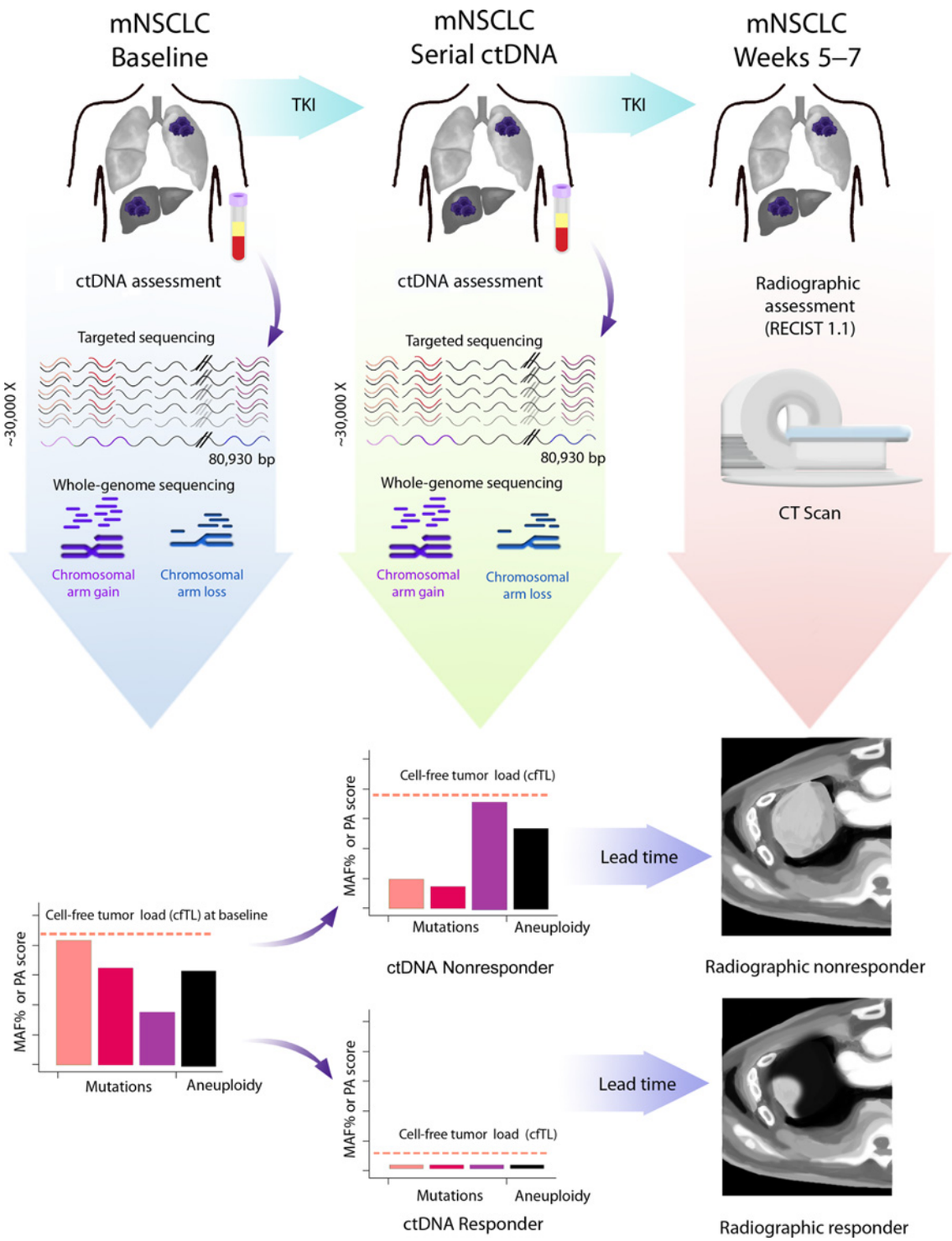

Figure 1.
Schematic of cfTL determination and prediction of therapeutic response. Liquid biopsies from metastatic non–small cell lung cancer (mNSCLC) patients undergoing treatment with tyrosine kinase inhibition were analyzed at baseline and at serial time points after treatment. The TEC-Seq approach was used to directly identify sequence alterations across 58 genes encompassing 80,930 bases sequenced to >30,000× coverage, and whole-genome approaches were used to identify copy number changes in cfDNA. The cfTL was determined as the mutant allele fraction of the most abundant alteration in a clone targeted by TKI for patients with detected sequence alterations, or as the presence or absence of aneuploidy based on PA score in patients without detectable sequence alterations. Prediction of therapeutic response to targeted therapy based on ctDNA dynamics was assessed through changes in cfTL from baseline to subsequent timepoints post treatment, whereas response assessment through CT imaging was performed 5–7 weeks after treatment.

Table 1. Baseline clinicopathologic features

Characteristics	
Number of patients	28
Median age (min–max)	57 (48–84)
Gender	
Male	9 (32.1%)
Female	19 (67.9%)
Stage at diagnosis	
I	2 (7.1%)
II	4 (14.3%)
III	3 (10.7%)
IV	19 (67.9%)
Smoking status	
Former	6 (21.4%)
Never	22 (78.6%)
Median pack-years (min-max)	15 (8–23)
Histopathologic diagnosis	
Adenocarcinoma	26 (92.8%)
Squamous cell carcinoma	1 (3.6%)
Mixed	1 (3.6%)
Metastastic sites	
Lung	15 (53.6%)
Bone	12 (42.9%)
Brain	11 (39.3%)
Liver	7 (25.0%)
Current treatment	
Osimertinib	15 (53.6%)
Afatinib	5 (17.9%)
Mavelertinib (PF-06747775)	5 (17.9%)
Erlotinib	3 (10.7%)
Previous treatment	
Anti-EGFR agent	20 (71.4%)
Chemotherapy	11 (39.3%)
Immune checkpoint blockade	1 (3.6%)
Brain radiation	5 (17.9%)

samples as well as not present in a custom database of common germline variants derived from dbSNP; (iv) the altered base did not arise from misplaced genome alignments including paralogous sequences; and (v) the mutation fell within a protein-coding region and was classified as a missense, nonsense, frameshift, or splice site alteration.

Candidate alterations were defined as somatic hotspots if the nucleotide change and amino acid change were identical to an alteration observed in $\geq$20 cancer cases reported in the COSMIC database. Alterations that were not hotspots were retained only if either (i) seven or more distinct paired reads contained the mutation in the plasma and the number of distinct paired reads containing a particular mutation in the plasma was at least 0.1% and less than 0.2%, of the total distinct read pairs or (ii) six or more distinct paired reads contained the mutation in the plasma and the number of distinct paired reads containing a particular mutation in the plasma were at least 0.2% of the total distinct read pairs. To track clonal changes over time, any alteration identified in at least one blood draw was assessed in the remaining timepoints.

Common germline variants were identified and removed if present in $\geq$25% of reads or <25% of reads if the variant was recurrent and the majority of alterations at that position had a mutant allele fraction $\geq$ 25%. Variants known to be at a somatic hotspot position or producing a truncating mutation in a tumor suppressor gene were not excluded as germline changes. Because of the high frequency of mutations in specific genes and the possible confounding between somatic and germline changes, we limited analyses in the *APC* gene to frameshift or nonsense mutations, and in *KRAS*, *HRAS*, and *NRAS* to positions to 12, 13, 61, and 146. Finally, we excluded hematopoietic expansion–related variants that have been described previously (29–33), including those in *DNMT3A*, *IDH1*, and *IDH2* and specific alterations within *ATM*, *GNAS*, *JAK2*, or *TP53* (Supplementary Table S3).

Primary processing of next-generation sequencing data for analyses of copy number alterations in cfDNA samples was performed as follows: Bam files were preprocessed by successively running CleanSam and MarkDuplicates from Picard Tools version 2.9.0. (http://broadinstitute.github.io/picard). Sequence reads were aligned against the human reference genome (hg19) using NovoAlign.

Candidate somatic structural variants were identified through analyses of low-coverage whole-genome sequencing data obtained from off-target reads mapping outside of the targeted capture of 58 cancer driver genes (Supplementary Table S3) in areas of the genome farther than 1,000 base pairs from the start or end of a targeted region. Off-target reads were divided into 100-kb bins with the exception of filtered bins (i) with less than 10 kb due to spacing of target regions, (ii) having GC content less than 30% or greater than 70%, (iii) where 25% fell within the ENCODE Duke Excluded Regions Track (http://genome.ucsc.edu/cgi-bin/hgFileUi?db=hg19&g=wgEncodeMapability). The total number of unique reads mapping to each bin were counted to exclude filtered regions:

$$s_b = \log_2\left(\frac{100000}{x_b - f_b} \times r_b\right)$$

where r_b is the number of unique reads mapped to bin b, x_b is the length of bin b, and f_b is the number of filtered base pairs within bin b, and the normalized score, s_b, was assigned to each bin. To remove GC-bias and normalize for sequencing depth, we used LOESS smoothing to predict a bin's normalized score from the bin-specific GC content. The GC-corrected score for each bin, $\widetilde{s_b}$, is defined for bin b by subtracting the predicted score from s_b and exponentiating this using base 2. We summed the GC-corrected scores for each chromosome arm. The summed score for a given chromosome arm was divided by the summed score using all bins to calculate the percentage of genomic representation.

Z scores were calculated as described previously (10) for each chromosome arm for each timepoint and patient assessed to determine areas of genome over or under representation. PA scores were calculated as described previously (10) using the five chromosome arms with the largest absolute z scores. PA scores higher than the threshold score of 2.4 provide a specificity greater than 90% (Student *t* distribution, three degrees of freedom) for the presence of aneuploid circulating tumor DNA.

Cell-free tumor load

We directly detected sequence and copy number alterations in cfDNA for each patient at each timepoint analyzed and used a tiered approach to evaluate tumor burden. For patients with detectable sequence alterations, the mutant allele fraction of the most abundant alteration in a clone targeted by the TKI was used as readout of cfTL. In patients without detectable sequence alterations, we evaluated the PA score as a binary readout of cfTL where a score above 2.4 indicated aneuploidy and evidence of tumor burden and a score below 2.4 indicated

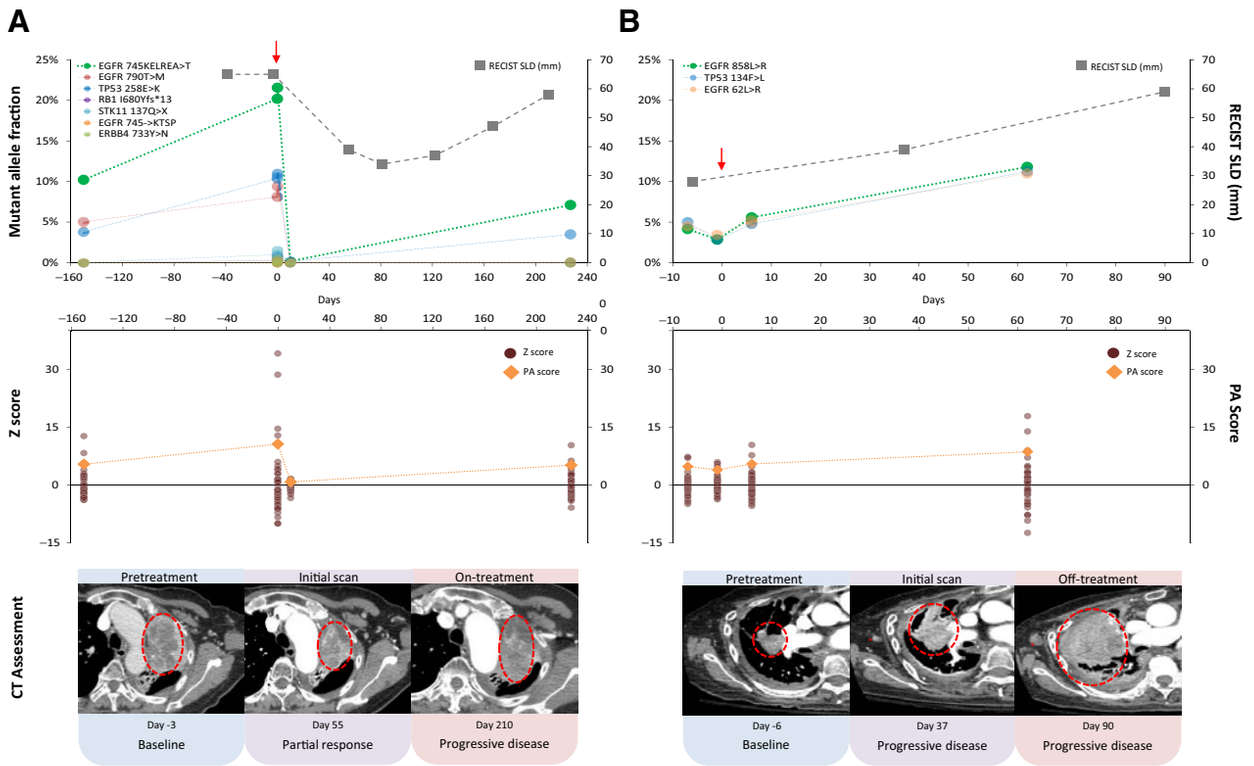

Figure 2.

Dynamic changes of ctDNA during therapy. Characteristic patterns of ctDNA changes during therapy are shown for a responder (CGPLLU12; **A**) and a nonresponder (CGPLLU244; **B**), both treated with osimertinib. Mutant allele fractions of clones identified in cfDNA through the TEC-Seq approach are shown for each timepoint analyzed with the ctDNA clone representing cfTL (bright green) and treatment initiation (red arrow; top). Copy number changes identified in cfDNA from analyses of whole-genome data are shown at each timepoint analyzed as Z scores (burgundy dots) for each chromosome arm and PA scores (orange diamonds; middle). RECIST 1.1 sum of longest diameters (SLD, gray boxes) were measured from CT scans at intervals during therapy (top) and CT images show representative tumor lesions for each patient circled in red (bottom).

normal ploidy and the absence of detectable tumor burden in plasma.

Changes in cfTL were evaluated to compare tumor burden at baseline and at other timepoints during treatment using quantitative assessment of cfTL mutant allele fractions for patients with detectable sequence clones and qualitative assessment of change from aneuploidy to normal ploidy representing a complete response for patients without detectable sequence clones (Fig. 3A and B; Supplementary Fig. S2).

Analyses of concordance between alterations observed with TEC-Seq in the plasma and clinical NGS analyses in the tumor tissue or plasma were performed for alterations within overlapping panel regions (Supplementary Fig. S3). Alterations identified through TEC-Seq, but not evaluated with clinical NGS analyses of tumor tissue or plasma, were not assessed for concordance.

Statistical analysis

Significance was determined using a variety of methods. To assess the significance of reduction in cfTL (Fig. 3A), change in the number of sequence mutations detected (Fig. 3B), and reduction in PA scores (Supplementary Fig. S2), and in patients with radiographic response or stable disease versus patients with no radiographic response posttreatment we used the Wilcoxon signed rank test. The significance of newly emerging mutations in 6 of 8 patients within the same day after initiation of therapy were evaluated by comparison with emerging alterations in 2 patients detected at earlier timepoints within 188 days prior to therapy. The rates of emerging mutations in the presence (within 4–12 hours) and absence of selective pressure of therapy were compared using a Gamma-Poisson Bayesian model. A Gamma (1, 100) prior was used for both mutation rates. Reported rates were based on the posterior mean and 99% posterior credible intervals (CI; Fig. 4). We compared progression-free survival in ctDNA responders versus ctDNA nonresponders (Fig. 5C) as well as in RECIST subgroups (partial response, stable disease, and progressive disease; Supplementary Fig. S4) using the Mantel–Cox log-rank test. Paired *t* test was used to assess the difference in the time to response assessment posttherapy based on ctDNA analyses versus RECIST (Fig. 5D).

Results

Overall approach

As a proof of concept, we evaluated cell-free DNA (cfDNA) from 28 patients with advanced non–small cell lung cancer. Of the 28 patients, 9 were initially diagnosed with stage IA, IIA, or IIIA disease, and the remaining presented with metastatic disease at initial diagnosis (Table 1). Prior to these analyses, patients

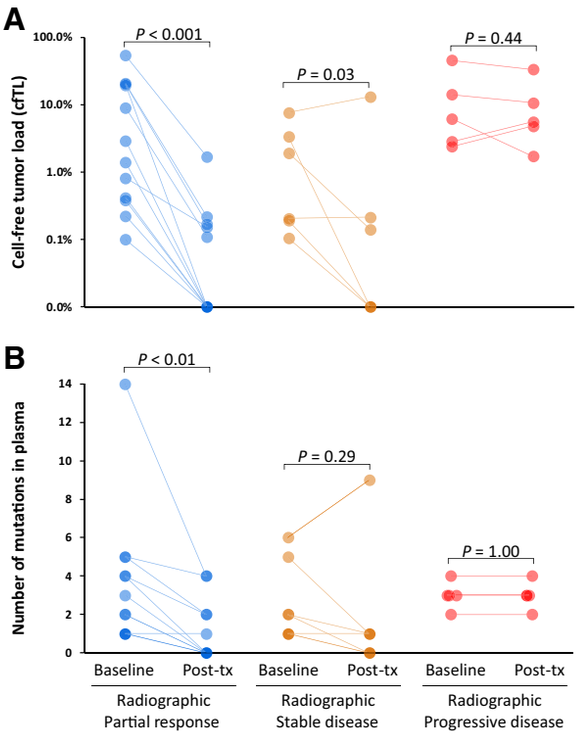

Figure 3.

Characteristics of cell-free DNA in patients treated with tyrosine kinase inhibitors. Changes in cfTL (**A**) and the number of mutations in plasma (**B**) in patients with partial response (blue), stable disease (orange), and progressive disease (red) from baseline to the time of ctDNA assessment after initiation of therapy. The partial response subgroup also included two patients with nonmeasureable disease by RECIST who were classified as clinical responders.

received treatment with anti-EGFR agents ($n = 20$), platinum-based chemotherapy ($n = 11$), or immune checkpoint inhibitors ($n = 1$; Table 1; Supplementary Table S1). Nine patients initially treated with first- or second-generation EGFR TKIs developed the *EGFR* T790M resistance mutation and were subsequently treated with third-generation EGFR TKIs (Supplementary Table S1). We performed liquid biopsy analyses during treatment with targeted therapies, including osimertinib ($n = 15$), afatinib ($n = 5$), mavelertinib ($n = 5$), or erlotinib ($n = 3$; Supplementary Table S1).

Tumor response for these patients was determined using RECIST version 1.1 (27). Of the 28 patients analyzed, 12 achieved a partial response based on their initial CT assessment after treatment initiation, while 8 patients exhibited stable disease, and five developed progressive disease (Supplementary Table S1). One patient with limited miliary metastases in the lungs and two with exclusive bone lesions were classified as having nonmeasurable disease (Supplementary Table S1).

For each patient, approximately 5 mL of plasma were collected immediately prior to therapy (baseline), at a median time of 19 days after therapy initiation, and at additional serial timepoints until disease progression was confirmed by radiographic assessment (Supplementary Tables S1 and S2). To analyze changes in cfDNA in these patients and capture the clonal heterogeneity of metastatic disease, we developed a combined comprehensive approach for analysis of both sequence and chromosomal changes. For sequence analyses, we used our recently developed TEC-Seq approach to evaluate 58 well-known cancer driver genes (Fig. 1; Supplementary Tables S3–S5; ref. 6). This method is based on targeted capture and deep sequencing (>30,000×) of DNA fragments to provide a high degree of specificity across 80,930 bp of coding gene regions and enables identification of tumor-specific alterations in ctDNA while distinguishing these from amplification and sequencing artifacts, germline changes, or alterations related to blood cell proliferation that may be present in cfDNA (6). To evaluate chromosomal changes that may be present in ctDNA, we used whole-genome sequences obtained from off-target fragments that were not captured during analysis of targeted regions in manner similar to other genome-wide copy number analyses, including Digital Karyotyping and related NGS approaches (10, 34, 35). The most aberrant alterations in the genome representation of individual chromosome arms were used to construct a plasma aneuploidy score (PA score) that was evaluated to detect changes in ctDNA during therapy (Supplementary Table S6).

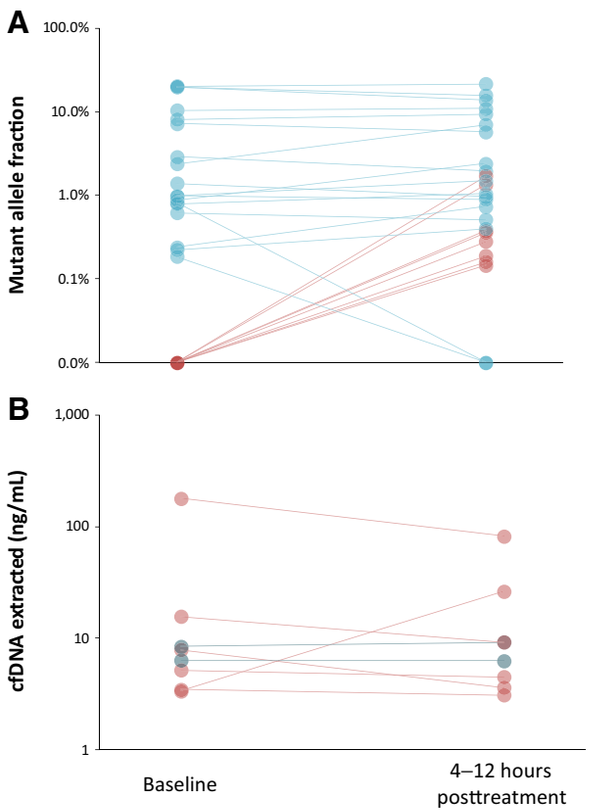

Figure 4.

Detection of ctDNA variants within hours after tyrosine kinase inhibitor initiation. Changes in the levels of ctDNA (**A**) as well as of cfDNA extracted (**B**) are depicted for 8 patients at baseline and at 4 to 12 hours after the initiation of targeted therapy. Emerging ctDNA alterations and the corresponding cfDNA amounts for patients with these alterations are depicted in red.

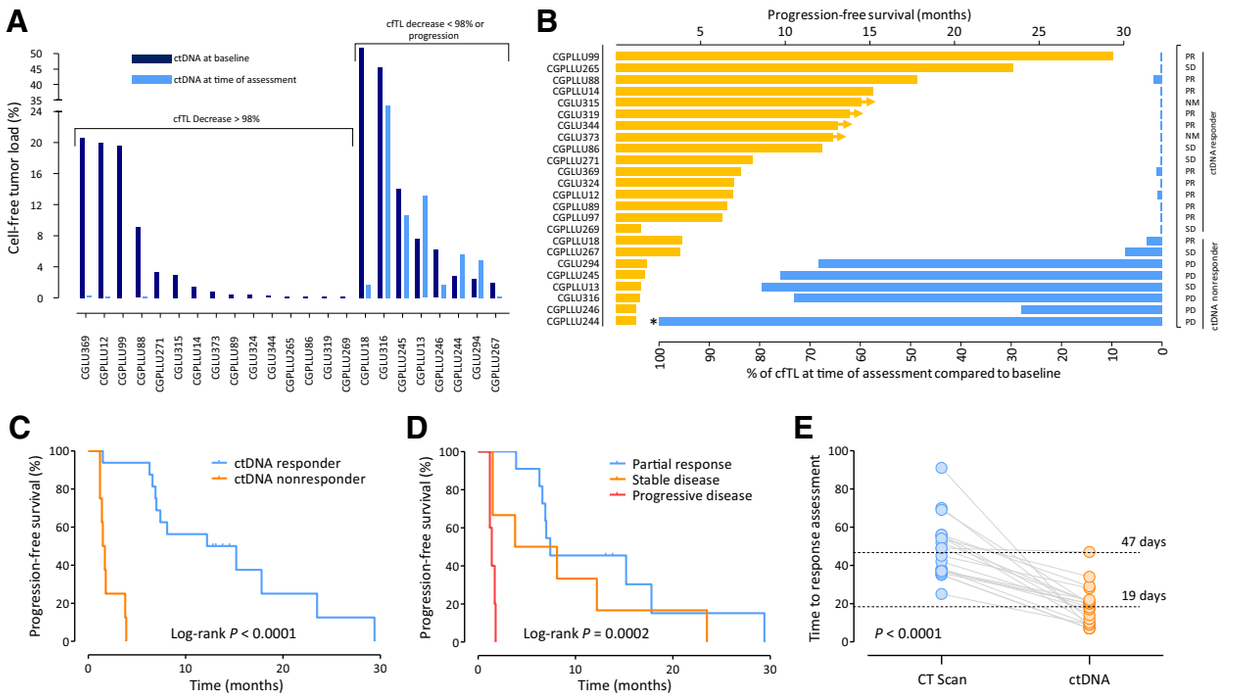

Figure 5.

Changes in ctDNA and prediction of response to therapy. **A,** Changes in cfTL from baseline to the time of ctDNA assessment revealed a bimodal distribution. Patients with reduction of cfTL >98% and ≤98% were categorized as ctDNA responders and ctDNA nonresponders, respectively. **B,** cfTL at the time of ctDNA assessment (blue) and PFS (orange) are depicted for patients analyzed. Radiographic assessment is indicated in the right column as partial response (PR), stable disease (SD), nonmeasurable disease (NM), or progressive disease (PD). Patient CGPLLU244 had cfTL levels >100% at the time of ctDNA assessment (*). **C,** Progression-free survival for ctDNA responders and nonresponders ($P < 0.0001$, Mantel–Cox log-rank test). **D,** Progression-free survival based on initial radiographic assessment ($P = 0.0002$, Mantel–Cox log-rank test). **E,** Time to response assessment as determined by CT scans (blue) or analyses of ctDNA (orange) are indicated with median time to assessment shown in dotted lines ($P < 0.0001$, Wilcoxon signed rank test).

Dynamics of cell-free tumor load

We evaluated ctDNA in all patients at baseline (pretreatment) and after the initiation of therapy. In the blood draws that were analyzed, we detected sequence alterations in 24 of 28 cases. At the baseline timepoint, patients had an average of 3.2 tumor-specific somatic mutations, affecting 16 driver genes, ranging from one to 14 alterations per case (Supplementary Table S5). Of 24 patients with detectable sequence alterations, 23 had at least one targetable mutation in either *EGFR* or *ERBB2*, with ctDNA mutant allele fractions ranging from 0.10% to 53.71% (Supplementary Table S5). Nine of the 15 patients treated with osimertinib had *EGFR* T790M acquired resistance mutations in the circulation at baseline, with ctDNA mutant allele fractions ranging from 0.13% to 10.09% (Supplementary Table S5), consistent with their previous treatment with EGFR TKIs (Supplementary Table S1). Previously described alterations in genes involved in blood cell proliferation (29–33) were observed in 18 patients across all timepoints analyzed, and were removed from further analyses (Supplementary Table S7). Chromosomal changes were detected in 18 of 28 cases analyzed. In most patients, multiple chromosomal arms were aberrant (Fig. 2; Supplementary Fig. S1; Supplementary Table S6), resulting in PA scores ranging from 2.6 to 14.9 at the baseline blood sample. Through our combined analyses, we identified either a tumor-derived sequence or chromosomal change or both types of alterations in 25 of 28 cases.

On the basis of the alterations observed in cfDNA through analyses of multiple genes, we developed a new metric, termed cell-free tumor load (cfTL), which is defined as the contribution of the most abundant alterations in cfDNA at any particular timepoint during the course of tumor evolution (Fig. 1; Supplementary Tables S5 and S6). In this study, the most abundant alterations were typically in driver genes targeted by the TKIs utilized (e.g., *EGFR* and *ERBB2*). We used a tiered approach to evaluate ctDNA levels, first using cfTL levels based on sequence changes, and then PA scores based on chromosomal changes if sequence alterations were not present. This approach has the benefit of providing a comprehensive assessment of tumor-derived alterations that would represent overall tumor burden during the course of disease and selective pressure of therapeutic interventions.

All patients with an initial objective radiographic response to targeted therapy displayed dramatic reduction of cfTL with mutant allele concentrations reduced from an average of 10.80% at baseline to 0.18% at a median time of 19 days after treatment initiation (>95% decrease, $P < 0.001$, Wilcoxon signed rank test; Figs. 2 and 3; Supplementary Fig. S1; Supplementary Table S1). Figure 2 depicts a representative patient with metastatic disease (CGPLLU12) who had a rapid decline of cfTL from baseline to day 10 after initiation of osimertinib. This patient exhibited a progression-free survival of 7.0 months, then subsequently developed resistance in the primary lung lesion. In

patients with radiographic stable disease, mutant allele concentrations were reduced from an average of 2.24% at baseline to 1.04% after treatment initiation (Fig. 3A; Supplementary Table S5; $P = 0.03$, Wilcoxon signed rank test). Likewise, PA scores decreased in responders (average decrease of 92%, $P = 0.002$, Wilcoxon signed rank test), including in patient CGPLLU97 who had no sequence alterations detected in the plasma (Supplementary Fig. S2). In contrast, all 5 patients with radiographic progressive disease experienced limited variation in cfTL, as measured through both sequence and chromosomal alterations, ranging from an average mutant allele fraction of 14.23% at baseline to 11.84% after initiation of therapy (Figs. 2 and 3A and B; Supplementary Fig. S1; $P = 0.6$, Wilcoxon signed rank test).

In addition to changes in cfTL, the average number of observed alterations also decreased in responders from 3.6 to 1.1 mutations per patient ($P < 0.01$, Wilcoxon signed rank test), while patients with stable or progressive disease had no significant change in the number of mutations observed during therapy (Fig. 3B). Clinical NGS testing performed to identify alterations in tumor tissue or plasma during the care of these patients independently confirmed 79.2% of the changes detected in our study (Supplementary Fig. S3). These observations suggest that both ctDNA levels and clonal heterogeneity are dramatically reduced at early timepoints in responding patients due to therapeutic selective pressure, and in nonresponding patients, the emergence and growth of tumor subclones can be detected earlier than radiographic progression.

Analysis of cfDNA within hours of therapy

For a subset of patients, we evaluated multiple follow-up blood draws at extremely early timepoints in therapy. An immediate timepoint within the same day at 4–12 hours after the initiation of the first dose of treatment was available for five patients who experienced a radiographic partial response on the first or second scan (CGPLLU12, CGPLLU14, CGPLLU86, CGPLLU99, and CGLU344), two clinical responders classified with nonmeasurable disease (CGLU315 and CGLU373), and one patient with progressive disease (CGLU294). In 6 of the 8 patients for whom immediate timepoints were evaluated, increasing ctDNA levels allowed for the identification of eight tumor-derived alterations not previously detected at baseline, including the targetable *EGFR* 746ELREATS>D clone in patient CGPLLU86 and an *EGFR*-resistance mutation T790M in patient CGLU344 (Fig. 4A). Mutant allele fractions of the newly detected clones ranged from 0.15% to 1.70% with an average of 0.57% and suggested that these alterations were likely below the limit of detection at baseline and were detected due to an increase in ctDNA levels. Evaluating the relative rate of emerging mutations in a Bayesian statistical model, we estimated a 110-fold increase in the rate of emerging mutations comparing posttreatment to pretreatment levels (99% CI: 13–732). Overall, cfDNA amounts remained relatively constant between baseline and timepoints 4–12 hours after treatment, indicating that changes in ctDNA levels occurred due to changes in the relative abundance of mutated clones within cfDNA (Fig. 4B). These observations suggest that the emergence of novel ctDNA variants may be related to early effects of therapy and are consistent with studies showing BIM-mediated apoptosis in responsive tumors 6–48 hours after exposure to EGFR inhibitors (36, 37).

Cell-free tumor load and clinical outcome

We evaluated whether the dynamic cfTL changes observed at early timepoints after treatment initiation were associated with differences in clinical outcome. cfTL levels at these early time points were bimodal, with the lower group clustering at an average reduction in cfTL of 99.8% and the higher group having an average increase in cfTL of 0.06% (Fig. 5A). We defined ctDNA responders as those with reduction in cfTL levels within three standard deviations of average reduction of the lower group (greater than 98.4%) while nonresponders were below this threshold. Eight of 12 patients who developed a complete ctDNA response (cfTL reduction of 100%) experienced progression-free survival longer than 1 year (Fig. 5B; Supplementary Figs. S4 and S5). Of the 6 patients with radiographic stable disease, ctDNA analyses identified four patients with a molecular response (average PFS of 11.3 months) and two molecular nonresponders (average PFS of 2.6 months). One patient who was a radiographic partial responder but a molecular nonresponder had a PFS of 3.9 months. Importantly, 2 patients with nonmeasurable disease by RECIST were clearly identified as molecular responders with an average PFS of 13.7 months. Overall, we observed a significantly shorter median progression-free survival for ctDNA nonresponders compared with ctDNA responders (1.6 months vs. 13.7 months, $P < 0.0001$; HR = 66.6; 95% CI: 13.0–341.7, log-rank test; Fig. 5C; Supplementary Fig. S5). Importantly, cfTL reduction at a median of 19 days appeared to be a more accurate predictor of clinical outcome compared with initial CT imaging performed an average of 47 days after initiation of therapy ($P < 0.0001$, Wilcoxon signed rank test; Figs. 5C–E; Supplementary Figs. S4–S6).

Discussion

Despite the success of targeted therapies for many cancers, durable responses eventually lead to progressive disease through the evolution of resistant clones. The standard approach for assessing treatment efficacy has been based on imaging measurement of tumor dimensions (27), which may not capture changes in clonal subpopulations and may be confounded by the tumor microenvironment. More recently, ctDNA methods have been used for disease monitoring, but these have largely been based on technologies that evaluate a limited number of genes or specific mutations and do not allow for evaluation of the dynamics of multiple tumor clones (9–18). We have developed an approach for evaluating tumor burden through a cell-free tumor load measurement that incorporates both sequence changes across many driver genes as well as whole-genome structural changes, allowing detection of tumor-related alterations in all patients analyzed. This effort addresses the value of comprehensive measurements of ctDNA within hours to days after targeted therapy initiation. In a complementary study, we have shown the benefit of these analyses for predicting response to immune checkpoint blockade using ctDNA dynamics (38).

Through this approach, we demonstrate that dynamic changes in plasma ctDNA after drug exposure may provide insights into clinical efficacy of targeted therapy. We observed a reduction of cell-free tumor load in patients with radiographic response and limited changes in ctDNA in nonresponders after initiation of therapy. We also showed that patients with radiographic nonmeasurable disease and those with stable disease at first imaging evaluation can be more accurately classified using ctDNA analyses after TKI initiation. These examples reflect the utility of ctDNA for

addressing current unmet clinical needs for real-time biomarkers of response and evolution of tumor burden. Although individual mutation analyses may miss specific subclones or may be absent in individual patients, the integrated analysis of sequence and structural changes permitted evaluation of the majority of cases for cfTL changes. The tiered complementary approach has the benefit of incorporating sequence mutations in cfDNA that have both qualitative and quantitative characteristics in the type and level of detected alterations, while chromosomal changes add quantitative assessment of genome-wide alterations that are typically present in every cancer.

Despite the clinical utility of this approach, these analyses have a number of limitations. First, our genome-wide analyses were based on whole-genome data at low coverage (<1×) and these could be improved in the future through deeper complementary sequencing. In addition, the cohort analyzed in this study was small and may not reflect the full repertoire of the disease complexity of patients with advanced NSCLC. Larger studies will be needed to validate these observations for patients with lung cancer treated with these and other targeted therapies, as well as for patients with other cancer types. Prospective trials with blood samples collected at regular intervals would allow for standardization of liquid biopsy analyses and for evaluation of responses to treatment compared with CT imaging.

Analysis of extremely early timepoints within hours after initiation of therapy identified the emergence of new tumor-derived mutations in most responding patients. The detection of new mutations and increase in the levels of existing alterations at this time provide insight into rapid release of ctDNA observed during apoptotic cell death. These analyses open the possibility of extremely early detection of response to targeted therapies. Faster and predictive determinants of patient response can aid in navigating adaptive therapeutic strategies to reduce toxicity, identify early resistance to targeted therapy, and enable the consideration of combinatorial approaches early in a patient's therapy. In addition, as occurred in 2 patients, these data indicate the utility of a single dose of treatment to elicit levels of ctDNA high enough to identify possible tumor-derived alterations.

These results suggest a new paradigm in cancer therapeutics and drug development in which cfTL molecular response criteria may be used to provide insight into clinical endpoints including overall survival and progression-free survival. Given the heterogeneity of metastatic disease, the cfTL approach we describe has the advantage of measuring overall tumor burden of clonal populations during selective pressure of targeted therapies. For patients without molecular response, liquid or tissue biopsies can provide additional information related to mechanisms of resistance and provide a context to consider other therapeutic strategies. cfTL monitoring may provide an early biomarker for proof-of-concept studies of novel targeted therapies both for established and new molecular targets. Combining cfTL response information with early pharmacokinetic data may ultimately provide the biologically effective dose needed for an individual's cancer rather than a maximally tolerated dose. Novel clinical trials could include rapid response assessments using cfTL in basket designs to expedite drug development.

Disclosure of Potential Conflicts of Interest

P.M. Forde reports receiving a commercial research grant from Bristol–Myers Squibb, AstraZeneca, Novartis, Kyowa, and Corvus and is a consultant/advisory board member for Abbvie, AstraZeneca, Bristol–Myers Squibb, Boehringer Ingelheim, EMD Serono, Inivata, Lilly, Merck, and Novartis. J. Naidoo reports receiving a commercial research grant from AstraZeneca/MedImmune, Merck, is a consultant/advisory board member for Bristol–Myers Squibb, AstraZeneca/MedImmune, Takeda, Genetech/Roche, and has provided expert testimony for Bristol–Myers Squibb and AstraZeneca/MedImmune. K.A. Marrone is a consultant/advisory board member for Takeda. J.R. Brahmer reports receiving a commercial research grant from Bristol–Myers Squibb and is a consultant/advisory board member for Bristol–Myers Squibb, Merck, Genentech, Amgen, Janssen, Syndax, Celgene, and AstraZeneca. D.N. Palsgrove is a pathology consultant at Personal Genome Diagnostics. V. Adleff is a consultant/advisory board member for Personal Genome Diagnostics. V.E. Velculescu has ownership interest (including stock, patents, etc.) in Personal Genome Diagostics and Ignyta and is a consultant/advisory board member for Personal Genome Diagostics and Ignyta. H. Husain reports receiving other commercial research support from Pfizer, AstraZeneca, Mirati, Astellas, has received speakers bureau honoraria from AstraZeneca, Merck, Bristol–Myers Squibb, and is a consultant/advisory board member for AstraZeneca, Boehringer Ingelheim, Abbvie, and Foundation Medicine. No potential conflicts of interest were disclosed by the other authors.

Authors' Contributions

Conception and design: J. Phallen, A. Leal, P.M. Forde, J. Naidoo, J.R. Brahmer, V.E. Velculescu, H. Husain

Development of methodology: J. Phallen, A. Leal, B.D. Woodward, V. Adleff, R.B. Scharpf, V.E. Velculescu, H. Husain

Acquisition of data (provided animals, acquired and managed patients, provided facilities, etc.): J. Phallen, A. Leal, B.D. Woodward, P.M. Forde, J. Naidoo, K.A. Marrone, J.R. Brahmer, J.E. Medina, C.D. Gocke, E. Weihe, H. Husain

Analysis and interpretation of data (e.g., statistical analysis, biostatistics, computational analysis): J. Phallen, A. Leal, B.D. Woodward, J.R. Brahmer, J. Fiksel, J.E. Medina, S. Cristiano, D.C. Bruhm, P. Keshavarzian, V. Anagnostou, R.B. Scharpf, V.E. Velculescu, H. Husain

Writing, review, and/or revision of the manuscript: J. Phallen, A. Leal, B.D. Woodward, P.M. Forde, J. Naidoo, K.A. Marrone, J.R. Brahmer, D.N. Palsgrove, C.D. Gocke, D.C. Bruhm, P. Keshavarzian, E. Weihe, V. Anagnostou, R.B. Scharpf, V.E. Velculescu, H. Husain

Administrative, technical, or material support (i.e., reporting or organizing data, constructing databases): J. Phallen, A. Leal, B.D. Woodward, V.E. Velculescu, H. Husain

Study supervision: J. Phallen, A. Leal, P.M. Forde, V.E. Velculescu, H. Husain

Acknowledgments

We thank members of our laboratories for critical review of the manuscript. We would like to thank Carolyn Hruban for help with artwork, and Ayesha Murtaza, Hannah Yang, Ajaz Bulbul, Fernando Lopez Diaz, Lyudmila Bazhenova, and William Mitchell for their contributions and thoughtful discussions. This work was supported in part by the Dr. Miriam and Sheldon G. Adelson Medical Research Foundation, the SU2C-DCS Dream Team Translational Cancer Research Grant (SU2C-AACR-DT1415), the Stand Up To Cancer-LUNGevity-American Lung Association Lung Cancer Interception Dream Team Translational Cancer Research Grant (SU2C-AACR-DT23-17), the Commonwealth Foundation, The Cigarette Restitution Fund, IASLC/Prevent Cancer Foundation, the Mark Foundation for Cancer Research, and US NIH grants CA121113, CA006973, CA180950, and CA193145. Stand Up To Cancer is a division of the Entertainment Industry Foundation. Research grants are administered by the American Association for Cancer Research, the Scientific Partner of SU2C. Data for this study have been deposited in the database of Genotypes and Phenotypes (dbGaP, study ID 33305).

The costs of publication of this article were defrayed in part by the payment of page charges. This article must therefore be hereby marked *advertisement* in accordance with 18 U.S.C. Section 1734 solely to indicate this fact.

Received April 11, 2018; revised September 4, 2018; accepted December 19, 2018; published first December 20, 2018.

References

1. Sawyers C. Targeted cancer therapy. Nature 2004;432:294–7.
2. Vogelstein B, Papadopoulos N, Velculescu VE, Zhou S, Diaz LA. Jr, Kinzler KW. Cancer genome landscapes. Science 2013;339:1546–58.
3. Haber DA, Velculescu VE. Blood-based analyses of cancer: circulating tumor cells and circulating tumor DNA. Cancer Discov 2014;4:650–61.
4. Newman AM, Bratman SV, To J, Wynne JF, Eclov NC, Modlin LA, et al. An ultrasensitive method for quantitating circulating tumor DNA with broad patient coverage. Nat Med 2014;20:548–54.
5. Bettegowda C, Sausen M, Leary RJ, Kinde I, Wang Y, Agrawal N, et al. Detection of circulating tumor DNA in early- and late-stage human malignancies. Sci Transl Med 2014;6:224ra24.
6. Phallen J, Sausen M, Adleff V, Leal A, Hruban C, White J, et al. Direct detection of early-stage cancers using circulating tumor DNA. Sci Transl Med 2017;9:pii: eaan2415.
7. Alix-Panabieres C, Pantel K. Clinical applications of circulating tumor cells and circulating tumor DNA as liquid biopsy. Cancer Discov 2016;6: 479–91.
8. Siravegna G, Marsoni S, Siena S, Bardelli A. Integrating liquid biopsies into the management of cancer. Nat Rev Clin Oncol 2017;14:531–48.
9. Diehl F, Schmidt K, Choti MA, Romans K, Goodman S, Li M, et al. Circulating mutant DNA to assess tumor dynamics. Nat Med 2008;14: 985–90.
10. Leary RJ, Sausen M, Kinde I, Papadopoulos N, Carpten JD, Craig D, et al. Detection of chromosomal alterations in the circulation of cancer patients with whole-genome sequencing. Sci Transl Med 2012;4:162ra54.
11. Diaz LA Jr, Williams RT, Wu J, Kinde I, Hecht JR, Berlin J, et al. The molecular evolution of acquired resistance to targeted EGFR blockade in colorectal cancers. Nature 2012;486:537–40.
12. Rago C, Huso DL, Diehl F, Karim B, Liu G, Papadopoulos N, et al. Serial assessment of human tumor burdens in mice by the analysis of circulating DNA. Cancer Res 2007;67:9364–70.
13. Tie J, Kinde I, Wang Y, Wong HL, Roebert J, Christie M, et al. Circulating tumor DNA as an early marker of therapeutic response in patients with metastatic colorectal cancer. Ann Oncol 2015;26:1715–22.
14. Leary RJ, Kinde I, Diehl F, Schmidt K, Clouser C, Duncan C, et al. Development of personalized tumor biomarkers using massively parallel sequencing. Sci Transl Med 2010;2:20ra14.
15. McBride DJ, Orpana AK, Sotiriou C, Joensuu H, Stephens PJ, Mudie LJ, et al. Use of cancer-specific genomic rearrangements to quantify disease burden in plasma from patients with solid tumors. Genes Chromosomes Cancer 2010;49:1062–9.
16. Garlan F, Laurent-Puig P, Sefrioui D, Siauve N, Didelot A, Sarafan-Vasseur N, et al. Early evaluation of circulating tumor DNA as marker of therapeutic efficacy in metastatic colorectal cancer patients (PLACOL Study). Clin Cancer Res 2017;23:5416–25.
17. Yanagita M, Redig AJ, Paweletz CP, Dahlberg SE, O'Connell A, Feeney N, et al. A prospective evaluation of circulating tumor cells and cell-free DNA in EGFR-mutant non-small cell lung cancer patients treated with erlotinib on a phase II trial. Clin Cancer Res 2016;22:6010–20.
18. Pecuchet N, Zonta E, Didelot A, Combe P, Thibault C, Gibault L, et al. Base-position error rate analysis of next-generation sequencing applied to circulating tumor DNA in non-small cell lung cancer: a prospective study. PLoS Med 2016;13:e1002199.
19. Dawson SJ, Tsui DW, Murtaza M, Biggs H, Rueda OM, Chin SF, et al. Analysis of circulating tumor DNA to monitor metastatic breast cancer. N Engl J Med 2013;368:1199–209.
20. Abbosh C, Birkbak NJ, Wilson GA, Jamal-Hanjani M, Constantin T, Salari R, et al. Phylogenetic ctDNA analysis depicts early-stage lung cancer evolution. Nature 2017;545:446–51.
21. Paweletz CP, Sacher AG, Raymond CK, Alden RS, O'Connell A, Mach SL, et al. Bias-corrected targeted next-generation sequencing for rapid, multiplexed detection of actionable alterations in cell-free DNA from advanced lung cancer patients. Clin Cancer Res 2016;22:915–22.
22. De Greve J, Teugels E, Geers C, Decoster L, Galdermans D, De Mey J, et al. Clinical activity of afatinib (BIBW 2992) in patients with lung adenocarcinoma with mutations in the kinase domain of HER2/neu. Lung cancer 2012;76:123–7.
23. Sequist LV, Yang JC, Yamamoto N, O'Byrne K, Hirsh V, Mok T, et al. Phase III study of afatinib or cisplatin plus pemetrexed in patients with metastatic lung adenocarcinoma with EGFR mutations. J Clin Oncol 2013;31: 3327–34.
24. Shepherd FA, Rodrigues Pereira J, Ciuleanu T, Tan EH, Hirsh V, Thongprasert S, et al. Erlotinib in previously treated non-small-cell lung cancer. N Engl J Med 2005;353:123–32.
25. Mok TS, Wu YL, Ahn MJ, Garassino MC, Kim HR, Ramalingam SS, et al. Osimertinib or platinum-pemetrexed in EGFR T790M-positive lung cancer. N Engl J Med 2017;376:629–40.
26. Janne PA, Yang JC, Kim DW, Planchard D, Ohe Y, Ramalingam SS, et al. AZD9291 in EGFR inhibitor-resistant non-small-cell lung cancer. N Engl J Med 2015;372:1689–99.
27. Schwartz LH, Litiere S, de Vries E, Ford R, Gwyther S, Mandrekar S, et al. RECIST 1.1-Update and clarification: from the RECIST committee. Eur J Cancer 2016;62:132–7.
28. Jones S, Anagnostou V, Lytle K, Parpart-Li S, Nesselbush M, Riley DR, et al. Personalized genomic analyses for cancer mutation discovery and interpretation. Sci Transl Med 2015;7:283ra53.
29. Xie M, Lu C, Wang J, McLellan MD, Johnson KJ, Wendl MC, et al. Age-related mutations associated with clonal hematopoietic expansion and malignancies. Nat Med 2014;20:1472–8.
30. Wong TN, Ramsingh G, Young AL, Miller CA, Touma W, Welch JS, et al. Role of TP53 mutations in the origin and evolution of therapy-related acute myeloid leukaemia. Nature 2015;518:552–5.
31. Genovese G, Kahler AK, Handsaker RE, Lindberg J, Rose SA, Bakhoum SF, et al. Clonal hematopoiesis and blood-cancer risk inferred from blood DNA sequence. N Engl J Med 2014;371:2477–87.
32. Shih AH, Chung SS, Dolezal EK, Zhang SJ, Abdel-Wahab OI, Park CY, et al. Mutational analysis of therapy-related myelodysplastic syndromes and acute myelogenous leukemia. Haematologica 2013;98:908–12.
33. Jaiswal S, Fontanillas P, Flannick J, Manning A, Grauman PV, Mar BG, et al. Age-related clonal hematopoiesis associated with adverse outcomes. N Engl J Med 2014;371:2488–98.
34. Heitzer E, Ulz P, Belic J, Gutschi S, Quehenberger F, Fischereder K, et al. Tumor-associated copy number changes in the circulation of patients with prostate cancer identified through whole-genome sequencing. Genome Med 2013;5:30.
35. Wang TL, Maierhofer C, Speicher MR, Lengauer C, Vogelstein B, Kinzler KW, et al. Digital karyotyping. Proc Natl Acad Sci U S A 2002;99:16156–61.
36. Costa DB, Halmos B, Kumar A, Schumer ST, Huberman MS, Boggon TJ, et al. BIM mediates EGFR tyrosine kinase inhibitor-induced apoptosis in lung cancers with oncogenic EGFR mutations. PLoS Med 2007;4: 1669–79.
37. Gong Y, Somwar R, Politi K, Balak M, Chmielecki J, Jiang X, et al. Induction of BIM is essential for apoptosis triggered by EGFR kinase inhibitors in mutant EGFR-dependent lung adenocarcinomas. PLoS Med 2007;4:e294.
38. Anagnostou V, Forde PM, White JR, Niknafs N, Hruban C, Naidoo J, et al. Dynamics of tumor and immune responses during immune checkpoint blockade in non-small cell lung cancer. Sci Transl Med 2018.